Hyperspectral predictors for monitoring biomass production in Mediterranean mountain grasslands: Majella National Park, Italy

M.A. CHO*
Council for Scientific and Industrial Research, Natural Resources and the Environment Unit Ecosystems Earth Observation Research Group. P.O. Box 395, Pretoria 0001, South Africa.– email: mcho@csir.co.za

A.K. SKIDMORE
International Institute for Geo-information Science and Earth Observation (ITC), Hengelosestraat, 99, P.O. Box 6, 7500 AA. Enschede, The Netherlands – email: skidmore@itc.nl

Abstract. The research objective was to determine robust hyperspectral predictors for monitoring grass/herb biomass production on a yearly basis in the Majella National Park, Italy. HyMap images were acquired over the study area on 15 July 2004 and 4 July 2005. The robustness of vegetation indices and red-edge positions (REP) were assessed by: (i) comparing the consistency of the relationships between green grass/herb biomass and the spectral predictors for both years and (ii) assessing the predictive capabilities of linear regression models developed for 2004 in predicting the biomass of 2005 and vice versa. Frequently used normalised difference vegetation indices (NDVI) computed from red (665-680 nm) and near-infrared bands, modified soil adjusted index (MSAVI), soil adjusted and atmospherically resistant index (SARVI) and water difference vegetation index (NDWI) were highly correlated with biomass ($R^2 \geq 0.50$) only for 2004 when the vegetation was in the early stages of senescence. Although high correlations ($R^2 \geq 0.50$) were observed for NDVI involving far-red bands at 725 and 786 nm for 2004 and 2005, the predictive regression model for each year produced a high prediction error for the biomass of the other year. Conversely, predictive models derived from REPs computed by the three-point Lagrangian interpolation and linear extrapolation methods for 2004 yielded a lower prediction error for the biomass of 2005, and vice versa, indicating these approaches are more robust than NDVI. The results of this study are important for selecting hyperspectral predictors for monitoring annual changes in grass/herb biomass production in the Mediterranean mountain ecosystems.

1. Introduction

Monitoring grass biomass through time can provide important information about the stability of natural ecosystems and whether significant changes are taking place (Jensen, 2000). This could be relevant particularly in mountain environments because of the sensitivity of these systems to climate change. Remote sensing techniques have been widely used to model the spatial and temporal variability of grass biomass over large areas (Richardson *et al*. 1982, Everitt *et al.* 1989, Anderson *et al.* 1993, Wylie *et al.* 2002, Lu, 2006).

There are major limitations with the normalised difference vegetation index (NDVI) despite its wide application for modelling the spatio-temporal variations of biomass. NDVI (Rouse *et al.* 1974) is commonly computed from canopy reflectance in the red and near-infrared (NIR) using broad-band imagery such as NOAA advanced very high resolution radiometer (AVHRR). Several studies show that broad-band NDVI can be unstable, varying with soil colour, canopy structure, leaf optical properties and atmospheric conditions (Huete and Jackson, 1988, Middleton, 1991, Kaufman and Tanré, 1992, Qi *et al.* 1995, Todd *et al.* 1998). It has also been demonstrated that empirical models derived from NDVI are highly site and sensor specific and therefore unsuitable for application to large areas or in different seasons (Curran, 1994; Gobron *et al*. 1997).

Furthermore, broad-band NDVIs asymptotically approach a saturation level after a certain biomass or leaf area index (Sellers, 1985, Gao *et al*. 2000). Broad-band NDVIs use average spectral information over broad-band widths resulting in loss of critical information available in specific narrow-bands (Blackburn, 1998, Thenkabail *et al.* 2000).

Recent developments in hyperspectral remote sensing have provided additional bands (narrow-bands) within the red-NIR transition that have been utilised to improve grass biomass estimation. For example, Mutanga and Skidmore (2004) show that NDVI computed from 746 and 755 nm solves the saturation problem of estimating grass biomass at high canopy cover. Another hyperspectral predictor that has been assessed for grass biomass estimation is the wavelength of maximum slope in the red-NIR region, termed the red-edge position (REP) (e.g. Gilabert *et al.* 1996, Mutanga and Skidmore,2004, Cho et al, in press). An advantage of the REP over the NDVI is that it is less sensitive to varying soil and atmospheric conditions, and sensor view angle (Curran *et al.* 1995, Blackburn and Pitman, 1999, Clevers *et al.* 2001). Many recent studies assessing the utility of hyperspectral predictors for estimating grass biomass have focused on single crops or species canopies (Thenkabail et al. 2000, Hansen and Schjoerring 2003, Mutanga and Skidmore 2004). The utility of hyperspectral predictors for estimating or monitoring biomass in natural grass and/or herb communities remains to be established.

The Mediterranean mountain grasslands in the region of Abruzzo, Italy consist of mixed grass/herb communities (Conti, 1998). These systems attain peak biomass in summer. But the hot summer climate, and variable cloud presence and precipitation in the region imply that the vegetation and atmospheric conditions are not stable. A major challenge in remote sensing of vegetation is the transferability of models developed at one time/place to another (Woodcock *et al.* 2001, Foody *et al*. 2003, Lu 2006). The monitoring of peak grass/herb biomass on an annual basis would require that the relationship between biomass and the spectral predictor remains stable for different summer atmospheric and vegetation conditions.

Thus, the research objective was to determine stable or robust hyperspectral predictors for estimating biomass production in Mediterranean mountain grasslands on a yearly basis. HyMap data was acquired in the study area, the Majella National Park, Italy in early and mid July 2004 and 2005, respectively. The robustness of vegetation indices and REP for monitoring grass/herb biomass was determined by: (i) comparing the consistency of the linear relations between biomass and hyperspectral predictors for 2004 and 2005 and (ii) assessing the predictive capabilities of empirical models developed for 2004 in predicting the biomass of 2005 and vice versa.

2. Material and methods

2.1. The study area

The study site is located in Majella National Park, Italy (latitude 41°52' to 42°14'N, longitude 13°50' to 13°14'E), which covers an area of 74095 ha. The park extends into the southern part of Abruzzo, at a distance of 40 km from the Adriatic Sea. This region is situated in the massifs of the Apennines (Conti, 1998). The park is characterised by several mountain peaks, the highest being Mount Amaro (2794 m).

More specifically, the study site (latitude 41°49’ to 42°14’N, longitude 13°57’ to 14°6’E) is situated between Mounts Majella and Morrone to the east and west, respectively. It covers an area of 40 km by 5.5 km. Gallego Fernández *et al*. (2004) argue that plant community dynamics in Mediterranean basin ecosystems are driven mainly by alternating episodes of human intervention and land abandonment. For example, abandoned settlement and agricultural areas in Majella are returning to oak (*Quercus pubescens*) woodlands at the lower altitude (400 m to 600 m) and beech (*Fagus sylvatica*) forest at the higher altitude (1200 m to 1800 m). Between these two formations is a landscape composed of shrubby bushes, patches of grass/herb vegetation, and bare rock outcrops.

The dominant grass species include *Brachypodium genuense*, *Briza media*, *Bromus erectus* and *Festuca sp*. Herbs include *Helichrysum italicum, Galium verum, Trifolium pratense, Plantago lanceolata, Sanguisorba officinalis* and *Ononis spinosa.*

2.2. Field data collection

Two field campaigns to collect grass/herb biomass data were carried out in the summers of 2004 (28 June to July 16) and 2005 (16 to 29 June). Random sampling with clustering was adopted in the study because of the difficult nature of the terrain. That is, twenty-five coordinate points were randomly generated with ArcGIS software from four phytosociological classes (semi-natural/farmlands, grazed/periodically flooded areas, open garrigue and abandoned farmlands): eight plots in the semi-natural/farmlands/abandoned farmlands, five plots in the open garrigues and twelve plots in the grazed/periodically flooded areas. The number of samples per vegetation class was proportional to the size of the class. To each plot, an extra plot was sampled about 150m away in a randomly chosen direction. The direction of the extra plot was randomly selected by throwing a piece of rock. Using a GPS, plots of 30 m by 30 m were located in the field. The plot size of 30m by 30m was deemed appropriate for the study area because of the spatial heterogeneity in vegetation types with autocorrelation distances of less than 50m. This fact notwithstanding, some plots fell within mixed grass/shrubby areas and such plots were sampled only when there was a patch of more than 20% of homogeneous and continuous fresh grass/herb cover. Twenty percent was chosen as the minimum area in such cases given that such an area could be conveniently captured within the HyMap image (spatial resolution of 4m). In general all plots were located in relatively homogenous areas in terms of grass/herb type and biomass. A total of 47 plots were sampled. All field sample plots were aligned in the direction of the flight line.

Above-ground biomass was clipped within five randomly selected subplots (1 m by 0.5 m) from each plot. All dry material was removed from the clipped plants before measuring the green biomass. Average green biomass per plot was calculated from the five subplot measurements.

2.3. Image acquisition and pre-processing

Airborne HyMap data of the study site were obtained on 15 July 2004 and 4 July 2005. The vegetation was greener in 2005 than in 2004 at the time of image acquisition. In addition, some parts of the study area were covered by clouds in 2005. The flights were carried out by DLR, Germany's Aerospace Research Centre and Space Agency. The HyMap sensor comprised 128 wavebands, operating over the wavelength range 436 nm to 2485 nm, with average spectral resolutions of 15 nm (436 nm to 1313 nm), 13 nm (1409 nm to 1800 nm) and 17 nm (1953 nm to 2485 nm). The spatial resolution of the data was 4 m. The data was collected at solar noon. The specific study site was covered by four image strips, each covering an area of about 40 km by 2.3 km. The solar zenith and azimuth angles for the image strips range between 30-33.7^{o} and 111.5-121^{o}, respectively.

The 2004 and 2005 image strips were atmospherically corrected by DLR. But only the 2005 images were geometrically corrected by DLR. The on-board navigation system used for geometric correction was a C-MIGITS II (Miniature Integrated GPS/INS Tactical System) system, which has a dx-dy accuracy of 2.5m and dz accuracy of 3m. The 2004 images strips were geometrically corrected from the 2005 images using image-to-image registration. The atmospheric correction was carried out using ATCOR4-r (Atmospheric/Topographic Correction-rugged terrain). ATCOR4 is based on MODTRAN-4 radiative transfer code (Richter and Schlapfer, 2002). However, there were differences between the reflectance of similar pixels in the overlapping sections between image strips for the 2005 image. We performed spectral calibration, using a reference image strip to mitigate the disparities. For example, image spectra collected from strip 2 (the reference strip) were used to correct its overlapping neighbours (strips 1 and 3). Ten pairs of spectra were collected from corresponding targets in the overlapping sections between strips 1 and 2 to correct strip 1 and another ten pairs between strips 2 and 3 to correct strip 3. The spectra were collected from targets such as roads, agricultural fields, quarry fields, and dense beech forest pixels. The spectra were then used to develop linear regression functions for each band. Using the regression functions, strips 1 and 3 were then adjusted to have a spectral response similar to that of strip 2. The same process was carried out using corrected strip 3 as the reference image to correct strip 4. The entire process was conducted using the empirical line tool in Environment for Visualising Images (ENVI 4.2) software (Research System, Inc.).

2.4. Collecting image spectra for grass/herb plots

Grass/herb areas were extracted from the image strips in order to eliminate mixed grass/shrubs and or tree pixels. First, an NDVI image involving bands at 665 nm and 831 nm was computed for each image strip using the ENVI 4.2 software. A point map of the grass/herb plots was then overlaid on the NDVI images. Pixels of pure grass/herb plots were used to determine minimum and maximum NDVI threshold values for grass/herbs. Next, a grass/herb region-of-interest map was created using the NDVI threshold values. Subsequently, the region-of-interest map was used to subset grass/herb areas from the image. All other pixels were masked out.

A 7 by 7 pixels window (i.e. 28m × 28m) was used to collect grass/herb image spectra from each sample plot in order to avoid including pixels located outside the plot (30 m × 30 m). The spectra were collected and averaged. The spectra of five out of the 47 plots were not extracted from the 2005 image strips because the plots were located in portions covered by clouds.

2.5. Data analysis

2.5.1. Spectral predictors

Two types of spectral predictors were adopted in this study:

[Insert Table 1]

(a) Vegetation indices

Four vegetation indices were used in the study: Narrow-band NDVI calculated from all combinations of red or far-red (600 to 740 nm) and NIR (756 to 1000 nm) bands, Modified soil adjusted vegetation index (MSAVI), soil and atmospherically resistant vegetation index (SARVI) and normalised difference water index (NDWI). The indices are presented in Table 1. Mutanga and Skidmore (2004) showed that widely used vegetation indices such as NDVI and transformed vegetation index (TVI) produce similar accuracies for grass biomass estimation. TVI was therefore not applied in this study.

(b) Red-edge position (REP)

Red-edge positions were extracted by three simple methods; the linear four-point interpolation (Guyot and Baret, 1988), three-point Lagrangian interpolation (Dawson and Curran, 1998) and the linear extrapolation (Cho and Skidmore, 2006) methods.

(i) Linear four-point interpolation method

The linear four-point interpolation method (Guyot and Baret, 1988) assumes that the reflectance curve at the red edge can be simplified to a straight line centred near the midpoint between the reflectance in the NIR at about 780 nm and the reflectance minimum of the chlorophyll absorption feature at about 670 nm. It uses four wavebands, 670, 700, 740 and 780 nm i.e. 665, 695, 740 and 786 for the HyMap spectrum. The REP is then determined by using a two-step calculation procedure.

Calculation of the reflectance at the inflexion point (R_{re}):

$$R_{re} = (R_{665} + R_{786})/2 \tag{1}$$

where R is the reflectance at a specified wavelength (e.g. 665 nm).

Calculation of the red edge wavelength or red edge position (REP):

$$\mathrm{REP} = 695 + 45\left(\frac{R_{re} - R_{695}}{R_{740} - R_{695}}\right) \tag{2}$$

695 and 45 are constants resulting from interpolation in the 695-740 nm interval.

(ii) Three-point Lagrangian interpolation method

The three-point Lagrangian interpolation technique (Dawson and Curran, 1998) is designed to locate REP in spectra that have been sampled coarsely. Lagrangian interpolation is applied to the first derivative of the reflectance spectrum which is computed as follows:

$$D_{(\lambda i)} = (R_{\lambda(j+1)} - R_{\lambda(j)})/\Delta\,\lambda \tag{3}$$

where $D_{(\lambda i)}$ is the first derivative reflectance at a wavelength i, midpoint between wavebands j and j+1, $R\lambda(j)$ is the reflectance at the j waveband, $R\lambda(j+1)$ is the reflectance at the j+1 waveband, and $\Delta\,\lambda$ is the difference in wavelengths between j and j+1.

The value of the first derivative at any wavelength (i.e. estimated value) will be D_λ. The Lagrangian interpolation technique for three known bands is given by

$$D_\lambda = \frac{(\lambda-\lambda_i)(\lambda-\lambda_{i+1})}{(\lambda_{i-1}-\lambda_i)(\lambda_{i-1}-\lambda_{i+1})}D_{\lambda(i-1)} + \frac{(\lambda-\lambda_{i-1})(\lambda-\lambda_{i+1})}{(\lambda_i-\lambda_{i-1})(\lambda_i-\lambda_{i+1})}D_{\lambda(i)} + \frac{(\lambda-\lambda_{i-1})(\lambda-\lambda_i)}{(\lambda_{i+1}-\lambda_{i-1})(\lambda_{i+1}-\lambda_i)}D_{\lambda(i+1)} \tag{4}$$

The band having the maximum first derivative will be λ_i, with λ_{i-1} and λ_{i+1} representing the two bands on either side of the maximum derivative. To determine the REP, a second derivation on Eq. 4 is performed and resolved for when the second derivative is zero. i.e.

$$\mathrm{REP} = \frac{A(\lambda_i + \lambda_{i+1}) + B(\lambda_{i-1} + \lambda_{i+1}) + C(\lambda_{i-1} + \lambda_i)}{2(A+B+C)} \tag{5}$$

where

$$A = \frac{D_{\lambda(i-1)}}{(\lambda_{i-1} - \lambda_i)(\lambda_{i-1} - \lambda_{i+1})}, B = \frac{D_{\lambda(i)}}{(\lambda_i - \lambda_{i-1})(\lambda_i - \lambda_{i+1})}, \text{and}$$
$$C = \frac{D_{\lambda(i+1)}}{(\lambda_{i+1} - \lambda_{i-1})(\lambda_{i+1} - \lambda_i)} \quad (6)$$

[Insert Fig. 1]

(iii) Linear extrapolation technique

The linear extrapolation technique (Cho and Skidmore, 2006) is designed to track changes near chlorophyll sensitive peaks in the first derivative (D) of the red edge i.e. around 700 and 725 nm (Horler *et al.* 1983). The REP is calculated as the wavelength at the intersection of two straight lines (Eq. 7 & 8) extrapolated through two points on the far-red flank and two points on NIR flank of first derivative reflectance spectrum. For example, for the HyMap derivative spectra used in this study, the lines were extrapolated through derivative bands at 672 and 703 nm for the far-red line and 732 and 778 nm for the NIR line (Fig. 1).

Far-red line: $D = m_1\lambda + c_1$ (7)

NIR line: $D = m_2\lambda + c_2$ (8)

where m and c represent the slope and intercept of the straight lines; m_1 and $c_1$for the far-red line and m_2 and c_2 for the NIR line. At the intersection, the two lines have equal λ and D values. Therefore, the REP, which is the λ at the intersection, is given by:

$$REP = \frac{-(c_1 - c_2)}{(m_1 - m_2)} \quad (9)$$

where

$$m_1 = \frac{(D_{703} - D_{672})}{(\lambda_{703} - \lambda_{672})} \quad (10)$$

$$m_2 = \frac{(D_{778} - D_{732})}{(\lambda_{778} - \lambda_{732})} \quad (11)$$

$$c_1 = D_{703} - m_1\lambda_{703} \quad (12)$$

$$c_2 = D_{732} - m_2\lambda_{732} \quad (13)$$

2.5.2. Assessing the robustness of hyperspectral predictors for monitoring grass/herb biomass

The robustness of the various spectral predictors for monitoring grass biomass was determined in two ways:

i the consistency of the linear regression models between biomass and the spectral predictors were compared for both 2004 and 2005. The explained variance (coefficient of determination or R^2) and prediction errors (the root mean square errors of leave-one-out cross-validation (RMSECV)) were used for the comparison (Geladi and Kowalski, 1986).

ii regression models developed for 2004 were used to predict the biomass of 2005 and vice versa. The performances of the various models for predicting either the next or previous years' biomass were compared using the standard errors of prediction (RMSE).

[Insert Table 2]
[Insert Fig. 2]

3. Results

3.1. Spectral and green grass/herb biomass characteristics for 2004 and 2005

The visible (450-700 nm), NIR (700-1300) and SWIR (1300-2500) reflectances were higher for 2004 than 2005 (Fig. 2). These results are consistent with changes that occur when vegetation loses pigmentation and water (Knipling, 1970), e.g. during the early stages of senescence. Furthermore, compared with 2005, the 2004 reflectance spectra showed higher variability (standard deviations) in the chlorophyll (600-700), and leaf/atmospheric water absorption (1450 and 1940 nm) bands (Curran, 1989).

The descriptive statistics for the green grass/herb biomass of 2004 and 2005 are presented in Table 2; the data distributions are assumed normal under the central limit theory. We used the 2-Sample Student's t-test to compute the confidence interval and perform a hypothesis test for the difference between the means of the biomass of 2004 and 2005. The null hypothesis was H_0: μ_1-μ_2 = 0 versus the alternative hypothesis H_1: μ_1-$\mu_2 \neq 0$, where μ_1 and μ_2 are the mean biomass of 2004 and 2005, respectively. The confidence interval (CI) for the difference in the means at 95% was -161, 149 g m^{-2}. The means were not significantly different at $p<0.05$. The annual variation in biomass calculated as the root of the mean square difference between the biomass of various plots for the two years was 334 g m^{-2}.

[Insert Tables 3 and 4]

3.2. Predictive performance of vegetation indices

The linear regression between grass/herb biomass and NDVIs computed from all combinations of wavebands between the NIR (756 to 1000 nm) and red or far-red (600 to 740 nm) produced different patterns for 2004 and 2005 (Fig. 3):

i in general, more combinations, i.e. 152 out of a total of 180 combinations yielded high coefficients of determination ($R^2 \geq 0.50$) for 2004 compared with 2005 (35 combinations)

ii the best five combinations for 2004 involved NIR bands and the red band at 695 nm, while for 2005, the best five combinations involved NIR bands and red-edge bands located at the longer wavelength end between 725 - 740 nm (Table 3)

iii the best five combinations for both 2004 and 2005 involved NIR bands located at the upper limit of the red edge (786 - 801 nm) and red-edge bands located mid-way along the red-edge slope (725 - 740 nm) (Table 4)

iv the more traditional NDVI band combinations involving NIR and red wavelengths around the chlorophyll absorption centre (660-680 nm) performed poorly for 2005 biomass estimation.

v The best five NDVI band combinations for 2005 are higher than those of 2004 (Table 3).

A comparative analysis of the predictive performance of the NDVI involving analogous Landsat TM bands (831 & 665 nm), best NDVI for 2004, best NDVI for 2005, overall best NDVI (786 & 725 nm), MSAVI, SARVI and NDWI is presented in Table 5. The MSAVI and SARVI provided an insignificant improvement over NDVI computed from red and NIR bands. NDWI produced a higher correlation for 2004 than 2005. Although NDVI (786 & 725 nm) and NDVI (786 & 740 nm) showed high correlations ($R^2 \geq 0.50$) and low RMSECV for both 2004 and 2005, they showed higher prediction errors for the following or previous years' biomass.

[Insert Fig. 3]

[Insert Table 5)

3.3. Predictive performance of the red-edge position

Among the REP methods, only REPs extracted by the Lagrangian and linear extrapolation methods were highly correlated ($R^2 \geq 0.50$) with biomass for 2004 and 2005. Nevertheless, REPs extracted by the linear interpolation method yielded the highest correlation ($R^2 = 0.62$) and lowest RMSECV (239 g m^{-2}) for 2005 when the vegetation was fresher. Compared with regression models developed using the best overall NDVI (786 & 725), the Lagrangian and linear extrapolation REP models for each year produced higher accuracies for grass/herb biomass prediction for the other year (Table 5 and Fig. 4). Figure 4 shows the predicted grass/herb biomass for a subset area of the 2005 image based on linear regression models derived from the best overall NDVI (786 & 725) and linear extrapolation REP for 2004 and 2005. This subset area represents the largest patch of grassland within the study area. The prediction has been applied on the original 4m pixel image given that resampling to the field plot size (30m) did not significantly change the results. This was expected because each plot was located in a relatively homogenous grass patch. It could be observed that the predicted maps based on the REP models showed higher similarities compared with the NDVI models.

[Insert Fig. 4]

4. Discussion

The present study evaluates the robustness or stability of hyperspectral predictors for estimating grass/herb biomass between two consecutive yearly hyperspectral images. HyMap data was acquired in the study area, the Majella National Park, Italy on 4 and 15 July 2004 and 2005, respectively. The spectral analyses of grass/herb plots (Fig. 2) seem to suggest that the vegetation and atmospheric conditions were different. However, no significant difference was found between the means of green grass/herb biomass for 2004 and 2005.

This study shows that frequently used NDVIs computed from canopy reflectance in the red (665-680 nm) and near-infrared bands, MSAVI, SARVI and NDWI are not reliable predictors of grass/herb biomass on a yearly basis. The above indices were highly correlated ($R^2 \geq 0.50$) with biomass only for 2004 when the vegetation was in the early stages of senescence. The greener vegetation of 2005 may have caused the saturation of traditional vegetation indices involving NIR bands and red bands between 670-690 (Mutanga and Skidmore, 2004). Conversely, the results do support the growing body of evidence which shows that narrow-bands in the red-edge are more consistent predictors of plant biophysical parameters (Thenkabail *et al.* 2000, Gupta *et al.* 2003, Hansen and Schjoerring 2003, Mutanga and Skidmore 2004). However, the linear regression models derived from the best overall NDVI involving narrow-bands at 786 and 725 nm were year-specific because the models for one year poorly predicted the biomass of another year. Differences in phenological and atmospheric conditions between 2004 and 2005 might have affected the stability or robustness of the empirically derived NDVI models. It has been shown in several other studies that empirical models derived from vegetation indices are highly site and sensor specific and unsuitable for application to large areas or in different seasons (e.g. Curran, 1994; Gobron *et al*. 1997).

The results of this study show that REPs extracted by the Lagrangian and linear extrapolation methods correlated highly ($R^2 \geq 0.50$) with green grass/herb biomass for both 2004 and 2005. Interestingly, the Lagrangian and linear extrapolation REP models for one year predicted the biomass of the other year with higher accuracies compared with the linear interpolation REP and NDVI (786 & 725 nm) regression models. Differences in phenological and atmospheric conditions might have only a minor effect on the relationship between biomass and the Lagrangian or linear extrapolation REP compared with the linear interpolation REP. In fact, Clevers *et al.* (2001) demonstrated that the REPs are least sensitive to atmospheric and soil conditions. This may apply particularly to the Lagrangian and linear extrapolation REPs which are computed from derivative spectra. Derivative analysis enhances absorption features and suppresses contributions of non-vegetative reflectance components (Boochs et al., 1990; Curran et al., 1991). The applicability of the Lagrangian and linear extrapolation REP regression models for different Mediterranean mountain grassland habitats and/or sensor types needs to be established.

In summary, the determination of spectral predictors that produce consistent correlations with peak grass/herb biomass for slightly different phenological and atmospheric conditions could be useful for monitoring annual changes in biomass production. These results are particularly crucial for the Mediterranean mountain landscape because of the unstable summer climate in this region, which makes it difficult to obtain cloud- or haze-free images at a desired phenological stage. Moreover, the robustness of regression models derived from the Lagrangian and linear extrapolation REPs, means that more reliable estimates of biomass can be obtained for a new HyMap image for which field-measured biomass data is unavailable. However, the results of this initial study on the robustness of hyperspectral indices in time/space are not conclusive as the study is based on only two consecutive years. Measurement for many more years shall be needed to draw more solid conclusion about the robustness of vegetation indices in time/space.

5. Summary and conclusions

The robustness of hyperspectral predictors for estimating green grass/herb biomass in the Majella National Park, Italy on a yearly basis were assessed in terms of (i) the consistency of the relationships between biomass and the spectral predictors and (ii) the capability of empirical models developed for 2004 to predict the biomass of 2005 and vice versa.

We conclude that the relationships between green grass/herb biomass and frequently used NDVIs computed from canopy reflectance in the red (665-680 nm) and near-infrared bands, MSAVI, SARVI and NDWI are not consistent from one year to the other. However, NDVI involving wavebands at 725 and 786 nm, or REPs extracted by the three-point Lagrangian interpolation and linear extrapolation techniques, produced high correlation ($R^2 \geq 0.50$) for both 2004 and 2005. However, the regression models based on REPs extracted by the Lagrangian and linear extrapolation methods for each year produced more reliable estimates of biomass for the other year.

The results of this study could be useful for selecting hyperspectral predictors for monitoring annual changes in grass/herb biomass production across other Mediterranean mountain ecosystems.

Acknowledgements

The International Institute for Geo-Information Science and Earth Observation (ITC) provided financial support for this study. We also extend our gratitude to the management of Majella National Park, Italy, and particularly to Dr Theodoro Andrisano.

References

ANDERSON, G.L., HANSON, J.D. and HAAS, R.H., 1993, Evaluating Landsat Thematic Mapper derived vegetation indices for estimating above-ground biomass on semiarid rangelands. Remote Sensing of Environment, **45**(2): 165-175.

BLACKBURN, G.A., 1998, Quantifying chlorophylls and caroteniods at leaf and canopy scales: An evaluation of some hyperspectral approaches. Remote Sensing of Environment, **66**: 273-285.

BLACKBURN, G.A. and PITMAN, J.I., 1999. Biophysical controls on the directional spectral reflectance properties of bracken (*Pteridium aquilinum*) canopies: results of a field experiment. International Journal of Remote Sensing, **20**(11): 2265-2282.

BOOCHS, F., KUPFER, G., DOCKTER, K. and KUHBAUCH, W., 1990, Shape of the red-edge as vitality indicator for plants. International Journal of Remote Sensing, **11**(10): 1741-1753.

CHO, M.A. and SKIDMORE, A.K., 2006, A new technique for extracting the red edge position from hyperspectral data: The linear extrapolation method. Remote Sensing of Environment, **101**(2): 181-193.

CHO, M.A., SKIDMORE, A.K., CHO, M.A., SKIDMORE, A.K., CORSI, F. van WIEREN, S.E. and SOBHAN, I. **(**in press). Estimation of green grass/herb biomass from airborne hyperspectral imagery using spectral indices and partial least squares regression. International Journal of Applied Earth Observation and Geoinformation

CLEVERS, J.G.P.W., DE JONG, S.M., EPEMA, G.F., VAN DER MEER F., BAKKER, W.H., SKIDMORE, A.K., and ADDINK, E.A., 2001, MERIS and the red-edge position. JAG, **3**(4): 313-319.

CONTI, F., 1998, Flora D'Abruzzo: An annotated checklist of the flora of the Abruzzo. Herbarium Mediterraneum Panormitanum, Palermo, Italy.

CURRAN, P.J., 1989, Remote sensing of foliar chemistry. Remote Sensing of Environment, **30**(3): 271-278.

CURRAN, P.J., 1994, Imaging spectrometry. Progress in Physical Geography, **18**(2): 247– 266.

CURRAN, P.J., DUNGAN, J.L., MACLER, B.A. and PLUMMER, S.E., 1991. The effect of a red leaf pigment on the relationship between red edge and chlorophyll concentration. Remote Sensing of Environment, **35**: 69-76.

CURRAN, P.J., WINDHAM, W.R. and GHOLZ, H.L., 1995, Exploring the relationship between reflectance red edge and chlorophyll concentration in slash pine leaves. Tree Physiology, **15**: 203-206.

DAWSON, T.P. and CURRAN, P.J., 1998, A new technique for interpolating red edge position. International Journal of Remote Sensing, **19**(11): 2133-2139.

EVERITT, J.H., ESCOBAR, D.E. and RICHARDSON, A.J., 1989, Estimating grassland phytomass production with near-infrared and mid-infrared spectral variables. Remote Sensing of Environment, **30**(3): 257-261.

FOODY, G.M., BOYD, D.S. and CUTLER, M.E.J. (2003) Predictive relations of tropical forest biomass from Landsat TM data and their transferability between regions, Remote Sensing of Environment 85, 463-474.

GALLEGO FERNÁNDEZ, J.B., GARCÍA MORA, M.R. and GARCÍA NOVO, F., 2004, Vegetation dynamics of Mediterranean shrublands in former cultural landscape at Grazalema Mountains, South Spain. Plant Ecology, **172**(1): 83-94.

GAO, B., 1996, NDWI - A normalized difference water index for remote sensing of vegetation water from space. Remote Sensing of Environment, **58**(3): 257-266.

GAO, X., HUETE, A.R., NI, W. and MIURA, T., 2000, Optical-biophysical relationships of vegetation spectra without background contamination. Remote Sensing of Environment, **74**: 609-620.

GELADI, P. and KOWALSKI, B.R., 1986. Partial least-squares regression: a tutorial. Analytica Chimica Acta, 185: 1-17.

GILABERT, M.A., GANDIA, S. and MELIA, J., 1996. Analyses of spectral-biophysical relationships for a corn canopy. Remote Sensing of Environment, **55**(1): 11-20.

GOBRON, N., PINTY, B. and VERSTRAETE, M.M., 1997, Theoretical limits to the estimation of the leaf area index on the basis of visible and near-infrared remote sensing data. IEEE Transactions on Geoscience and Remote Sensing, **35**(6): 1438– 1445.

GUPTA, R.K., VIJAYAN, D. and PRASAD, T.S., 2003, Comparative analysis of red-edge hyperspectral indices. Advance Space Research, **32**(11): 2217-2222.

GUYOT, G. and BARET, F., 1988, Utilisation de la haute résolution spectrale pour suivre l'état des couverts végétaux, Proceedings of the 4th International colloquium on spectral signatures of objects in remote sensing. ESA SP-287, Assois, France, pp. 279-286.

HANSEN, P.M. and SCHJOERRING, J.K., 2003, Reflectance measurement of canopy biomass and nitrogen status in wheat crops using normalized difference vegetation indices and partial least squares regression. Remote Sensing of Environment, **86**: 542-553.

HORLER, D.N.H., DOCKRAY, M. and BARBER, J., 1983, The red edge of plant leaf reflectance. International Journal of Remote Sensing, **4**(2): 273-288.

HUETE, A.R. and JACKSON, R.D., 1988, Soil and atmosphere influences on the spectra of partial canopies. Remote Sensing of Environment, **25**(1): 89-105.

JENSEN, J.R., 2000, Remote sensing of the environment: an earth resource perspective. Prentice Hall series in Geographic Information Science. Prentice Hall, New Jersey, 544 pp.

KAUFMAN, Y.J. and TANRÉ, D., 1992, Atmospherically resistant vegetation index (ARVI) for EOS-MODIS. IEEE Transactions on Geoscience and Remote Sensing, **30**(2): 261-270.

KNIPLING, E.B., 1970, Physical and physiological basis for the reflectance of visible and near-infrared radiation from vegetation. Remote Sensing of Environment, **1**: 155-159.

LU, D., 2006, The potential and challenge of remote sensing-based biomass estimation. International Journal of Remote Sensing **27**(7):1297-1328.

MIDDLETON, E.M., 1991. Solar zenith angle effects on vegetation indices in tallgrass prairie. Remote Sensing of Environment, **38**(1): 45-62.

MUTANGA, O. and SKIDMORE, A.K., 2004, Narrow band vegetation indices overcome the saturation problem in biomass estimation. International Journal of Remote Sensing, **25**: 1-16.

QI, J., CABOT, F., MORAN, M.S. and DEDIEU, G., 1995, Biophysical parameter estimations using multidirectional spectral measurements. Remote Sensing of Environment, **54**(1): 71-83.

RICHARDSON, A.J., WIEGAND, C.L., ARKIN, G.F., NIXON, P.R. and GERBERMANN, A.H., 1982, Remotely-sensed spectral indicators of sorghum development and their use in growth modeling. Agricultural Meteorology, **26**(1): 11-23.

RICHTER, R. and SCHLAPFER, D., 2002, Geo-atmospheric processing of airborne imaging spectrometry data. Part 2: atmospheric/topographic correction. International Journal of Remote Sensing, 23:2631-2649

ROUSE, J.W., HAAS, R.H., SCHELL, J.A., DEERING, D.W. and HARLAN, J.C., 1974, Monitoring the vernal advancement and retrogradation of natural vegetation, NASA/GSFC, Type III Final Report, M.D. Greenbelt, pp. 371.

SELLERS, P.J., 1985, Canopy reflectance, photosynthesis and transpiration. International Journal of Remote Sensing, **6**(8): 1335-1372.

THENKABAIL, P.S., SMITH, R.B. and DE PAUW, E., 2000, Hyperspectral vegetation indices and their relationships with agricultural crop characteristics. Remote Sensing of Environment, **71**: 158-182.

TODD, S.W., HOFFER, R.M. and MILCHUNAS, D.G., 1998, Biomass estimation on grazed and ungrazed rangelands using spectral indices. International Journal of Remote Sensing, **19**(3): 427-438.

WOODCOCK, C.E., MACOMBER, S.A., PAX-LENNEY, M. and COHEN, W.B., 2001, Monitoring large areas for forest change using Landsat: generalisation across space, time and Landsat sensors, Remote Sensing of Environment **78**, 194–203.

WYLIE, B.K., MEYER, D.J., TIESZEN, L.L. and MANNEL, S., 2002, Satellite mapping of surface biophysical parameters at the biome scale over the North American grasslands: A case study. Remote Sensing of Environment, **79**(2-3): 266-278.

Table 1
Summary of vegetation indices analysed in this study. R_{blue}, R_{red} *and* R_{NIR} denote reflectances in the blue, red and NIR, respectively.

Index	Formula	Description	References (e.g.)
NDVI	$(R_{NIR} - R_{red})/(R_{NIR} + R_{red})$	Normalised difference vegetation index. Related to changes in amount of green biomass and pigment content.	Rouse *et al*. 1974
MSAVI	$\frac{2R_{NIR}+1-\sqrt{(2R_{NIR}+1)^2-8(R_{NIR}-R_{red})}}{2}$	Modified soil adjusted vegetation index minimises soil influences on canopy spectra. Red and NIR bands at 665 nm and 831 nm, respectively.	Huete 1988, Qi *et al*. 1994.
SARVI	$R_{rb} = R_{red} - \gamma(R_{blue} - R_{red})$ The subscripts r and b denote the red and blue bands, respectively. γ denotes the atmospheric aerosol correction function. SARVI = $(R_{NIR} - R_{rb})/(R_{NIR} - R_{rb} + L)$ L = soil adjustment factor	Soil adjusted and atmospherically resistant vegetation index. Blue and red bands at 482 and 665 nm, respectively. $\gamma = 0.9$, $L = 0.5$	Kaufman and Tanre 1992, Huete *et al*. 1994.
NDWI	$(R_{860} - R_{1240})$ / $(R_{860} + R_{1240}$	Normalised difference water index is sensitive to changes in liquid water content of vegetation canopies. Gao (1996) showed that NDWI is less sensitive to atmospheric effects than NDVI	Gao 1996.

Table 2
Green grass/herb biomass data for 2004 and 2005 collected in Majella National Park, Italy

year	*N*	Mean ($g\ m^{-2}$)	SD	Minimum	Maximum
June/July 2004	47	768	366	200	1750
June 2005	42	774	369	210	2010

N = number of samples, SD = standard deviation

Table 3

Best NDVI combinations for predicting grass/herb biomass in the Majella National Park, Italy for 2004 and 2005. R^2 = coefficient of determination.

Near-infrared wavelength (nm)	Red or far-red wavelength (nm)	R^2
2004 HyMap image		
786	695	0.56
801	695	0.56
771	695	0.56
756	695	0.56
816	695	0.56
2005 HyMap image		
786	740	0.64
801	740	0.64
771	740	0.62
756	740	0.62
879	725	0.62

Table 4

Overall best NDVI combinations for predicting grass/herb biomass in the Majella National Park, Italy for both 2004 and 2005. They are classified according to decreasing difference in the coefficients of determination (R^2) between 2004 and 2005 for combinations that yielded high correlations ($R^2 \geq 50$) for both years.

Near-infrared wavelength (nm)	Red or far-red wavelength (nm)	R^2 2004	R^2 2005
786	725	0.55	0.58
801	725	0.54	0.59
756	740	0.51	0.62
771	740	0.51	0.62
786	740	0.50	0.64

Table 5

A comparative analysis of the performance of vegetation indices and red-edge position (REP) extracted by three methods for predicting grass/herb biomass using HyMap images. The images were acquired over Majella National Park, Italy in the summers of 2004 and 2005. R^2 and RMSECV denote the coefficient of determination and the root mean square error of leave-one-out cross validation, respectively.

2004 HyMap image	Linear regression model	R^2	RMSECV ($g\ m^{-2}$)	Prediction error (RMSE) based on 2005 model
NDVI (831 & 665 nm)	- 758.8 + 2328.7 NDVI	0.55	255	301
NDVI(786 & 695 nm)	- 455.7 + 2326.6 NDVI	0.56	252	298
NDVI (786 & 740 nm)	- 425 + 17522 NDVI	0.50	264	273
NDVI (786 & 725 nm)	- 205.1 + 5786.8 NDVI	0.55	252	294
MSAVI	- 1791.5 + 1627.5 MSAVI	0.54	258	304
SARVI	- 283.2 + 1847.6 SARVI	0.55	255	290
NDWI	804.69 + 5729.6 NDWI	0.55	251	389
REP (linear interpolation)	- 146667 + 205131 REP	0.47	272	352
REP (three-point Lagrangian interpolation)	- 52499 + 74475 REP	0.50	265	266
REP (linear extrapolation)	- 27980 + 40498 REP	0.53	258	279

2005 HyMap image	Linear regression model	R^2	RMSECV	Prediction error (RMSE) based on 2004 model
NDVI (831 & 665 nm)	- 744 + 2040.4 NDVI	0.32	319	361
NDVI(786 & 695 nm)	- 523 + 2121 NDVI	0.38	306	346
NDVI (786 & 740 nm)	- 697 + 20149 NDVI	0.64	231	349
NDVI (786 & 725 nm)	- 470.2 + 6393.5 NDVI	0.58	253	280
MSAVI	- 1703.4 + 1458.6 MSAVI	0.30	325	365
SARVI	- 270.5 + 1556.4 SARVI	0.31	322	356
NDWI	496.6 + 4866.4 NDWI	0.49	280	444
REP (linear interpolation)	- 181974+ 254570 REP	0.62	239	295
REP (three-point Lagrangian interpolation)	- 51651 + 73184 REP	0.56	258	254
REP (linear extrapolation)	- 33500 + 48110 REP	0.58	252	258

Note: All the relations were statistically significant at $p<0.05$

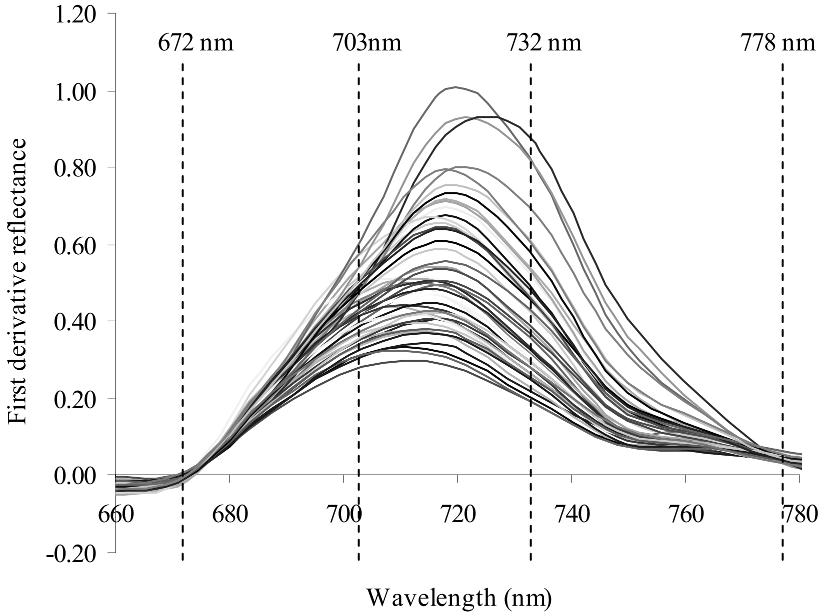

Figure 1. First derivative spectra of 2005 sample plots showing bands used in the calculation of red-edge positions by the linear extrapolation method.

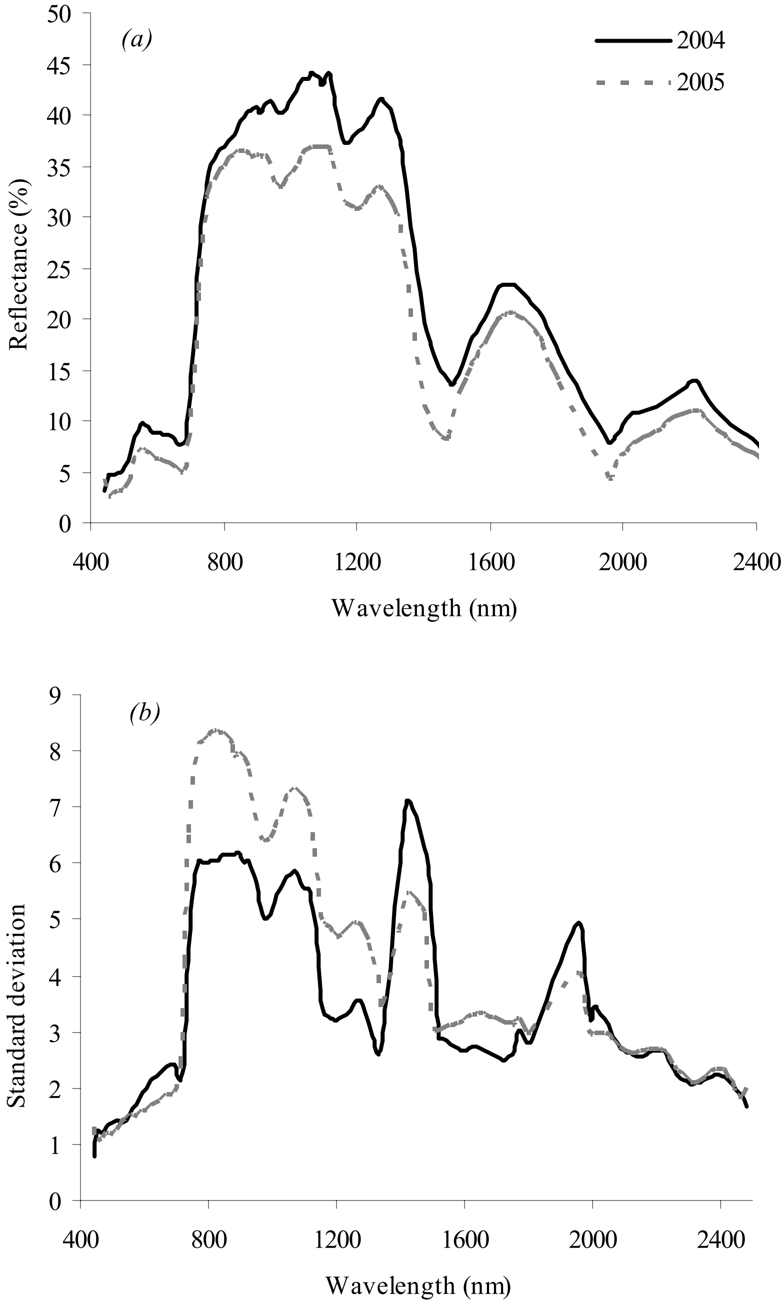

Figure 2. Mean reflectance spectra *(a)* and their corresponding standard deviations *(b)* for grass/herb plots extracted from HyMap images acquired over Majella National Park, Italy in mid and early July 2004 and 2005, respectively.

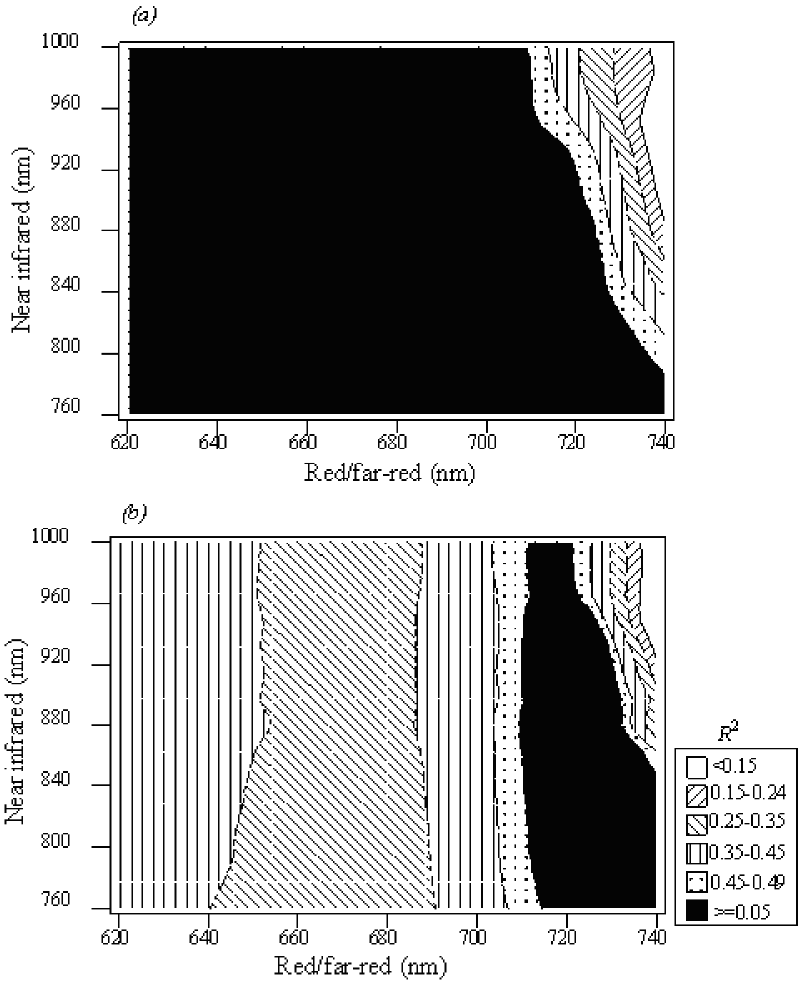

Figure 3. Contour plots showing the sensitivity (based on the coefficient of determination i.e. R^2) of the relations between Majella green grass/herb biomass and NDVIs calculated from all combinations of near-infrared (756 to 1000 nm) and red or far-red (600 to 740 nm) bands for *(a)* 2004 and *(b)* 2005 HyMap images.

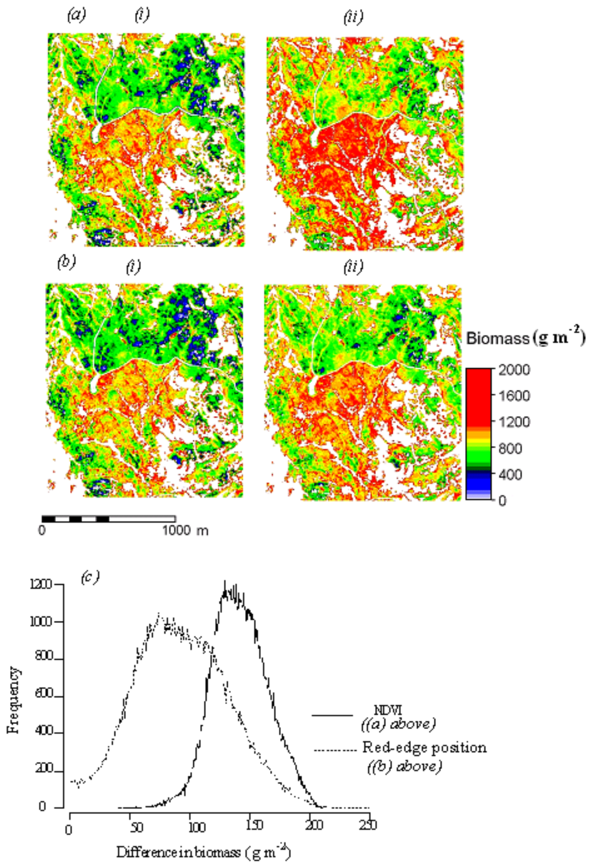

Figure 4. Predicted green grass/herb biomass for a subset area of the 2005 HyMap image based on *(i)* 2005 and *(ii)* 2004 regression models for *(a)* NDVI (786 & 725 nm) and *(b)* red-edge position extracted by the linear extrapolation method. *(c)* Histogram showing the differences between *(i)* and *(ii),* i.e. number of pixels against difference in biomass.